Acta Crystallographica Section B
Structural Science
ISSN 0108-7681

Structure-forming components in crystals of ternary and quaternary 3*d*-metal complex fluorides

E. V. Peresypkina and V. A. Blatov*

Samara State University, Ac. Pavlov Street 1, Samara 443011, Russia

Correspondence e-mail: blatov@ssu.samara.ru

Received 25 February 2003
Accepted 3 April 2003

Crystallochemical analysis and classification were performed for 139 ternary and quaternary complex fluorides with the general formula $M1_nM2_mM3F_6$, belonging to 33 structure types. Using coordination sequences and the uniformity criterion the structure-forming ionic sublattices or their combinations were found, which are responsible for the formation of stable periodic frameworks. Analysis of structure-forming motifs allows the interpretation of the crystal structures of complex fluorides as close packings of F ions with *M*1, *M*2 and *M*3 cations, partially occupying tetrahedral and octahedral voids, or as the packings of $[M3F_6]$ complex ions with *M*1 and *M*2 countercations in the voids. Cationic sublattices are noted to play an essential role, while forming crystal structures of complex fluorides. Relationships between the composition of structure-forming sublattices, the composition of compounds, and the size and charge of ions belonging to the sublattices were analysed under normal conditions, with thermal and high-pressure polymorphic transitions. Rules were formulated to predict the crystal structures of complex fluorides with a given chemical composition.

1. Introduction

At present 3*d* metal complex fluorides $M1_nM2_mM3F_6$, with countercations *M*1 and *M*2 and complexing ions *M*3, are well documented. The fluorides are known to form about 40 structure types; the same structure type usually occurs for compounds of similar stoichiometry, with a given ratio of radii of *M*1 and *M*2 ions. Thus, $M1_nM2_mM3F_6$ fluorides with $M1^{I}(M2^{I})$ = Li, Na form special structure types, as a rule, which do not occur for fluorides with large countercations $M1^{I}$ and $M2^{I}$ (Kemmitt *et al.*, 1963; Wells, 1986). In numerous structural investigations and reviews (Kemmitt *et al.*, 1963; Wells, 1986; Massa & Babel, 1988; Babel, 1967; Flerov *et al.*, 1998) the following empirical regularities were derived concerning structure types of complex fluorides:

(i) The structure types may be based on the packing of fluoride ions, the packing of both cations and anions, or the packing of complexes $[M3F_6]$.

(ii) The occurrence of a structure type is first determined by the size of the countercations, which are estimated with their ionic radii *r* and by the relative number of countercations (Babel, 1967; Wells, 1986). In particular, if the cations *M*1 or *M*2 (Li^{I}, Mg^{II}, Zn^{II} *etc.*) are smaller than the anions [$r(M1, M2) << r(F^{-})$], the crystal structures of complex fluorides are usually considered as the packing of fluoride ions with voids occupied by the *M*1, *M*2 and *M*3 cations (Babel, 1967; Courbion *et al.*, 1982; Wells, 1986; Sekino *et al.*, 1990). If the anions and some countercations are similarly sized, the crystal

Table 1
Topological properties and uniformity criterion values for ionic sublattices in inorganic 3*d* metal complex fluorides.

Topological properties for each structure type are given for anionic, complete cationic sublattices and for the sublattice of complexing atoms (*M*3), which also corresponds to the sublattice of [*M*3F$_6$] complex groups; if countercations are large, a mixed cationic–anionic sublattice is also taken into account. The G_3 range for ionic sublattices of the same topology is presented; G_3^{min} and G_3^{max} correspond to the minimum and maximum G_3 values for sublattices of the same topology in the group of compounds of the same structure type. Sequences of hexagonal (h) and cubic (c) closely packed layers are given in a footnote to this table.

Prototype	Compounds	Sublattice composition	Coordination sequence, $\{N_{1-3}\}$	$G_3^{min} - G_3^{max}$
Complex fluorides $M1_2M3F_6$				
Na_2SiF_6 (*P*32)	α-LiMnFeF$_6$	F$^-$	12, 44, 96	0.0794–0.0840
	NaMnCrF$_6$	*M*3^{III}	*M*3(1): 14, 44, 104	0.0791–0.0816
	LiTiMnF$_6$		*M*3(2): 11, 47, 98	
		*M*1^{I}, *M*3^{III}	*M*3(1): 15, 51, 122	0.0811–0.0815
			*M*3(2): 12, 46, 106	
			*M*1: 9, 41, 114	
			*M*2: 9, 47, 105	
Na_2SnF_6 (*P*2$_1$/*c*)	Li_2CrF_6	F$^-$	13, 49, 110	0.0818
monoclinic distortion of		*M*3^{IV}	12, 42, 92	0.0796
Na_2SiF_6		*M*1^{I}, *M*3^{IV}	10, 34, 74	0.0812
Na_2TiF_6 ($P\bar{3}m$)	Na_2TiF_6	F$^-$	12, 44, 96	0.0816–0.0822
	Li_2MnF_6	*M*3^{IV}	*M*3(1): 14, 44, 104	0.0791–0.0792
			*M*3(2): 11, 47, 98	
		*M*1^{I}, *M*3^{IV}	*M*1: 10, 40, 88	0.0875–0.0869
			*M*3(1): 8, 32, 80	
			*M*3(2): 12, 44, 92	
Na_2TiF_6 (*P*1)	Na_2TiF_6	F$^-$	12, 44, 96	0.0846
		*M*3^{IV}	*M*3(1): 14, 44, 104	0.0790
			*M*3(2,3): 11, 47, 98	
		*M*1^{I}, *M*3^{IV}	*M*1(1,2): 12, 41, 99	0.0809
			*M*1(3): 13, 41, 94	
			*M*1(4,5): 12, 44, 93	
			*M*1(3): 12, 42, 96	
			*M*3(1): 9, 37, 98	
			*M*3(2,3): 9, 43, 89	
K_2GeF_6 ($P\bar{3}m$)	K_2TiF_6	F$^-$	8, 28, 66	0.0884
		*M*3^{IV}	8, 26, 56	0.0817
		F$^-$, *M*1^{I}	12, 44, 96	0.0793
		*M*1^{I}, *M*3^{IV}	14, 50, 110	0.0802
K_2PtCl_6 ($Fm\bar{3}m$)	Cs_2CrF_6, Cs_2MnF_6	F$^-$	8, 30, 68	0.0868–0.0960
	Cs_2CoF_6, Cs_2NiF_6	F$^-$, *M*1^{I}	12, 42, 92	0.0788–0.0867
	Rb_2CrF_6, Rb_2CoF_6, Rb_2NiF_6	*M*3^{IV}	12, 42, 92	0.0788
	K_2CrF_6, K_2MnF_6	*M*1^{I}, *M*3^{IV}	*M*1: 10, 34, 82	0.0854–0.0862
			*M*3: 8, 36, 78	
(Rb,K)MnF$_6$ ($Fm\bar{3}m$)	(Rb,K)MnF$_6$ (Cs,Rb)MnF$_6$	F$^-$	8, 30, 68	0.0892–0.0909
derived from		F$^-$, *M*1^{I}	12, 42, 92	0.0809–0.0824
K_2PtCl_6		*M*3^{IV}	12, 42, 92	0.0788
		*M*1^{I}, *M*3^{IV}	*M*1: 10, 34, 82	0.0862
			*M*3: 8, 36, 78	
K_2MnF_6 (*P*6$_3$*mc*)	K_2MnF_6	F$^-$	F(1): 8, 30, 66	0.0897–0.0926
			F(2): 8, 28, 72	
	Rb_2MnF_6	F$^-$, *M*1^{I}	F(1), *M*1(2): 12, 42, 96	0.0804–0.0822
			F(2), *M*1(1): 12, 44, 96†	
		*M*3^{IV}	12, 44, 96	0.0788
		*M*1^{I}, *M*3^{IV}	*M*3(1): 14, 44, 104	0.0827–0.0829
			*M*3, *M*1(2): 11, 46, 98	
Cs_2VF_6 (*Ccmm*)	Cs_2VF_6	F$^-$	F(1): 9, 31, 73	0.0937
			F(2): 8, 31, 78	
			F(3): 8, 33, 70	
		F$^-$, *M*1^{I}	F(1): 12, 45, 104	0.0815
			F(2): 11, 41, 100	
			F(3),*M*1(1): 13, 49,102	
			*M*1(2): 13, 45, 104	
		*M*3^{IV}	10, 34, 74	0.0817
		*M*1^{I}, *M*3^{IV}	*M*3: 13, 50, 107	0.0805
			*M*1(1): 13, 48, 107	
			*M*1(2): 14, 48, 108	
Complex fluorides $M1_3M3F_6$				
Cryolite	Na_3ScF_6‡	F$^-$	F(1): 12, 42, 94	0.0807–0.0838
Na_3AlF_6 (*P*2$_1$/*c*)			F(2), F(3): 11, 49, 94	
	Na_3MnF_6, Na_3NiF_6, Na_3VF_6	*M*3^{III}	12, 42, 92	0.0788
		*M*1^{I}, *M*3^{III}	14, 50, 110	0.0790–0.0799
Cryolite	Na_3FeF_6	F$^-$	F(1), F(4): 12, 42, 94	0.0818
Na_3FeF_6 (*P*2$_1$)			F(2), F(3), F(5), F(6): 11, 42, 92	

Table 1 (continued)

Prototype	Compounds	Sublattice composition	Coordination sequence, $\{N_{1-3}\}$	$G_3^{min} - G_3^{max}$
		$M3^{III}$	12, 42, 92	0.0788
		$M1^{I}$, $M3^{III}$	14, 50, 110	0.0799
β-Li_3TiF_6 ($C2/c$)	β-Li_3TiF_6	F^-	F(1): 12, 43, 96 F(2): 12, 44, 96§	0.0794
		$M3^{III}$	$M3$(1): 14, 48, 108 $M3$(2): 13, 49, 106	0.0790
		$M1^{I}$, $M2^{I}$, $M3^{III}$	$M1$(1): 12, 44, 102 $M1$(2): 13, 49, 109 $M1$(3): 12, 46, 105 $M1$(4): 14, 48, 108 $M1$(5): 13, 47, 108 $M3$(1): 12, 46, 110 $M3$(2): 12, 47, 110	0.0807
Complex fluorides $M1M3F_6$				
$KOsF_6$ ($R\bar{3}m$)	$SrCrF_6$, $BaCrF_6$	F^-	11, 40, 90	0.0847–0.0861
derived from CsCl	$SrNiF_6$, $BaNiF_6$ $BSaTiF_6$	$M1^{II}$, F^-	$M1$: 14, 48, 116 F: 13, 49 113	0.0796–0.0802
		$M1^{I}$, $M3^{IV}$	14, 50, 110	0.0797–0.0802
		$M3^{IV}$	12, 44, 98	0.0816–0.0819
$LiSbF_6$ ($R\bar{3}$)	$CaCrF_6$, $MgCrF_6$	F^-	12, 44, 96	0.0805–0.0813
derived from NaCl	$HgCrF_6$, $CdCrF_6$	$M1^{II}$, $M3^{IV}$	6, 18, 38	0.0828–0.0832
	$CdTiF_6$	$M3^{IV}$	12, 42, 92	0.0788–0.0792
Complex fluorides $M1_2M2M3F_6$				
Cubic elpasolite (ordered perovskite)	Cs_2KM3F_6, $M3$ = Ti, V, Cr, Fe, Ni	F^-	8, 30, 68	0.0873–0.0911
		$M1^{I}$, F^-	12, 42, 92	0.0793–0.0826
K_2NaAlF_6 ($Fm\bar{3}m$)	Cs_2NaM3F_6, $M3$ = Sc, Mn, Fe	$M1^{I}$, $M2^{I}$, $M3^{III}$	14, 50, 110	0.0785
HP phase	Cs_2TlM3F_6, $M3$ = V, Fe Rb_2NaM3F_6, $M3$ = Ti, V, Cr, Fe, Ni, Co Rb_2KM3F_6, $M3$ = Sc, V, Cr, Fe, Ni, Co K_2NaM3F_6, $M3$ = Sc, Cr, Fe, Ni, Cu K_3M3F_6, $M3$ = Cr, Fe Tl_3TiF_6, Rb_3FeF_6	$M3^{III}$	12, 42, 92	0.0788
Tetragonally distorted cubic elpasolite	Cs_2KMnF_6	F^-	8, 30, 68	0.0898
Cs_2KMnF_6 ($F4/mmm$)		M^{I}, F^-	12, 42, 92	0.0815
		$M1^{I}$, $M2^{I}$, $M3^{III}$	14, 50, 110	0.0786
		$M3^{III}$	12, 42, 92	0.0788
Tetragonally distorted cubic elpasolite Rb_2KScF_6 ($I4/m$)	Rb_2KScF_6	F^-	F(1): 8, 30, 76 F(2): 8, 33, 76	0.0886
		$M1^{I}$, F^-	12, 42, 92	0.0810
		$M3^{III}$	12, 42, 92	0.0788
		$M3^{I}$, $M2^{I}$, $M3^{III}$	14, 50, 100	0.0785
Rombohedral elpasolite (ordered perovskite)	Cs_2NaCrF_6 Cs_2NaMnF_6 Cs_2NaFeF_6 Cs_2NaCoF_6 Cs_2NaNiF_6 Cs_2NaTiF_6 Rb_2LiFeF_6	F^-	F(1): 8, 29, 70 F(2): 8, 29, 66	0.0881–0.0939
Cs_2NaFeF_6 ($R\bar{3}m$)		$M1^{I}$, F^-	$M1$(1): 12, 44, 94 F(1): 12, 44, 94 $M1$(2): 12, 43, 96 F(2): 12, 43, 96¶	0.0793–0.0847
HT phase		$M3^{III}$	12, 42, 92	0.0788
		$M1^{I}$, $M2^{I}$, $M3^{III}$	$M1$ (1): 14, 47, 104 $M1$(2): 14, 50, 104 $M2$: 11, 47, 104 $M3$(1): 14, 44, 110 $M3$(2): 8, 44, 92	0.0802–0.0805
Trigonal elpasolite (ordered perovskite)	Cs_2NaTiF_6	F^-	F(1): 8, 30, 68 F(2): 8, 29, 69	0.0896
K_2LiAlF_6 ($P\bar{3}m$)		$M1^{I}$, F^-	$M1$(1), F(1): 12, 42, 92 $M1$(2), $M1$(3), F(2), F(3): 12, 43, 96††	0.0803
		$M3^{III}$	12, 42, 92	0.0788
		$M1^{I}$, $M2^{I}$, $M3^{III}$	$M1$ (1): 14, 47, 107 $M1$(2): 14, 50, 107	0.0796

Table 1 (continued)

Prototype	Compounds	Sublattice composition	Coordination sequence, $\{N_{1-3}\}$	$G_3^{min} - G_3^{max}$
			*M*1(3): 11, 50, 107 *M*2(1): 14, 44, 104 *M*2(2): 11, 47, 104 *M*3(1): 14, 44, 110 *M*3(2): 11, 47, 107	
Garnete $Li_3Na_3Fe_2F_{12}$ ($Ia\bar{3}d$)	$Li_3Na_3Fe_2F_{12}$	F^-	10, 40, 95	0.0819–0.0832
	$Li_3Na_3Co_2F_{12}$	$M3^{III}$	14, 50, 110	0.0785
	$Li_3Na_3Sc_2F_{12}$	$M1^I$, M^I, $M3^{III}$	*M*1, *M*2: 14, 50, 110	0.0787
	$Li_3Na_3V_2F_{12}$		*M*3: 12, 50, 110	
Complex fluorides $M1M2M3F_6$				
Modified pyrochlore $Rb(Ni,Cr)F_6$ ($Fd\bar{3}m$)	$Cs(Mn,V)F_6$, $Cs(Cu,M3)F_6$, *M*3 = Sc, Ti, V, Cr, Mn, Fe, Ni	F^- $M1^I$, F^-	8, 23, 54 *M*1: 18, 52, 162 F: 11, 50, 113	0.0949–0.0999 0.0824–0.0857
	$Cs(Ag,Sc)F_6$, $Cs(Ni,V)F_6$	$M1^I$, $M2^{II}$	6, 18, 48	0.0992
	$Cs(Co,M3)F_6$, *M*3 = V, Cr, Fe $Cs(Fe,M3)F_6$, *M*3 = V, Cr $Cs(Mg,M3)F_6$, *M*3 = Fe, Co, Ni $Cs(Mn,M3)F_6$, *M*3 = V, Cr, Fe $Cs(Ni,M3)F_6$, *M*3 = V, Cr, Fe $Cs(Zn,M3)F_6$, *M*3 = Fe, Co, Ni $K(Ni,Cr)F_6$, $Tl(Ni,Cr)F_6$, $Rb(Cu,M3)F_6$, *M*3 = Cr, Fe, Co $Rb(Mg,M3)F_6$, *M*3 = Cr, Co, Ni $Rb(Ni,M3)F_6$, *M*3 = Cr, Co $Rb(Zn,Co)F_6$	$M1^I$, $M2^{II}$, $M3^{III}$	*M*1: 16, 52, 130 *M*2, *M*3: 12, 50, 110	0.0793
$CsNi^{II}Ni^{III}F_6$ (*Imma*)	$CsNi^{II}Ni^{III}F_6$	F^-	8, 23, 54	0.0934–0.0962
Orthorhombically distorted ordered modified pyrochlore	$RbNi^{II}Ni^{III}F_6$	$M3^{III}$ $M1^I$, $M2^{II}$, $M3^{III}$	8, 26, 56 *M*2, *M*3: 12, 50, 110 *M*1: 16, 52, 130	0.0886–0.0893 0.0798–0.0800
Colquiriite $LiCaAlF_6$ ($P\bar{3}c$), ordered Li_2ZrF_6	$LiCaCrF_6$, $LiCaCoF_6$, $LiCaNiF_6$, $LiCdCoF_6$, $LiSrNiF_6$	F^- $M3^{III}$ $M1^I$, $M2^{II}$, $M3^{III}$	12, 44, 96 12, 44, 96 *M*1, *M*3: 9, 41, 72 *M*2: 12, 32, 90	0.0804–0.0817 0.0792–0.0799 0.0825–0.0832
Trirutile type, $(Li,Ni)CoF_6$) ($P4_2/mnm$	$(Li,Ni)CoF_6$, $(Li,Zn)CoF_6$, $(Li,Mg)CoF_6$, Li_2TiF_6	F^- $M3^{III}$ $M1^I$, $M2^{II}$, $M3^{III}$	13, 49, 110 12, 42, 92 10, 34, 74	0.0791–0.0792 0.0796–0.0798 0.0809–0.0813
$LiMnGaF_6$ (*P*32) closely related to Na_2SiF_6	β-$LiMnFeF_6$	F^- $M3^{III}$ $M1^I$, $M2^{II}$, $M3^{III}$	12, 44, 96 *M*3(1): 14, 44, 104 *M*3(2): 11, 47, 98 *M*1: 10, 38, 78 *M*2: 11, 35, 84 *M*3(1): 9, 35, 84 *M*3(2): 9, 38, 78	0.0795 0.0792 0.0814
$NaSrFeF_6$ ($P2_12_12_1$)	$NaSrFeF_6$	F^- $M3^{III}$ $M1^I$, $M2^{II}$, $M3^{III}$	12, 44, 96 12, 44, 96 *M*1: 12, 47, 113 *M*2: 15, 50, 111 *M*3: 9, 45, 108	0.0826 0.0789 0.0815
$LiSrCoF_6$ ($P2_1/c$), related to trirutile type	$LiSrCoF_6$	F^- $M3^{III}$ $M1^I$, $M2^{II}$, $M3^{III}$	F(1),(4): 11, 42, 95 F(2),(3): 12, 43, 95 F(5),(6): 12, 43, 94 12, 44, 96 *M*1, *M*3: 10, 47, 103 *M*2: 14, 44, 102	0.0820 0.0799 0.0832
$LiBaCoF_6$ ($P2_1/c$), related to trirutile type	$LiBaCoF_6$	F^- $M3^{III}$ $M1^I$, $M2^{II}$, $M3^{III}$	F(1): 10, 38, 87 F(2): 10, 40, 88 F(3): 10, 39, 89 F(4): 12, 41, 94 F(5): 12, 40, 93 F(6): 11, 40, 95 12, 44, 96 *M*1: 11, 48, 110 *M*2: 15, 48, 111 *M*3: 10, 48, 108	0.0853 0.0792 0.0805
$NaSrCrF_6$ ($P2_1/c$), related to trirutile type	$NaSrCrF_6$	F^- $M3^{III}$	F(1): 11, 41, 89 F(2),(6): 11, 40, 90 F(3): 11, 42, 91 F(4): 11, 41, 92 F(5): 11, 41, 91 12, 44, 96	0.0834 0.0791

Table 1 (continued)

Prototype	Compounds	Sublattice composition	Coordination sequence, $\{N_{1-3}\}$	$G_3^{min} - G_3^{max}$
		$M1^{I}$, $M2^{II}$, $M3^{III}$	*M*1: 11, 44, 113 *M2*: 15, 51, 111 *M3*: 10, 48, 116	0.0821

† 4L close packing (ch). ‡ The data on two crystal structure studies were analysed at normal and high pressures. § 9L close packing (chh). ¶ 12L close packing (chhc). †† 6L close packing (hcc).

structure is often represented as a packing of fluoride ions together with the countercations. Other cations occupy voids formed only by the anions (perovskite-like compounds; Wells, 1986). In most cases the mixed (cationic–anionic) packing comprises fluoride ions and sodium or potassium cations, since, according to different estimations, $r(K^+) \simeq r(F^-) \simeq$ 1.33–1.36 Å (Pauling, 1927; Bokii, 1971) and $r(Na^+) \simeq r(F^-) \simeq$ 1.13–1.16 Å (Shannon & Prewitt, 1969). Besides, one should take into account that if $6/n$ [or $6/(n+m)$] < 3, cationic–anionic packing cannot be realised because cations make contacts with each other (Wells, 1986). If a complex fluoride comprises only large countercations, and $r(M1)$, $r(M2) >> r(F^-)$, the crystal structure is usually described as a packing of the $[M3F_6]$ complex ions with the *M*1 and *M*2 countercations in the voids. Considering *M*3 as a complexing atom, some authors (*e.g.* Wells, 1986; Massa & Babel, 1988) pointed out the lack of direct relationships between crystal structures of complex fluorides and the nature and size of *M*3 cations, especially within the same transition series, because the size of complexes mainly depends on the ligand sizes. However, some additional secondary effects were observed (Babel, 1967; Wells, 1986; Massa & Babel, 1988; Englich & Massa, 1992; Gorev *et al.*, 1997; Flerov *et al.*, 1998).

(iii) The charge ratio for countercations predetermines the occurrence of ordered or disordered crystal structures. Some structure types, such as modified pyrochlore $Rb(Ni,Cr)F_6$, elpasolite K_2NaAlF_6 or trirutile, which are typical for quaternary complexes, are derived from the binary or ternary prototypes, namely, fluorite, perovskite and rutile, respectively. In this case a quaternary compound represents either the disordered or the superstructural prototype. The appearance of the superstructures or the structures with cationic disorder depends not only on the relative sizes of cations, but on their charges as well. Thus, similar sized cations of the same charge are crystallochemically indistinguishable and can replace one another to yield disordered fluorides (Babel, 1967). If the sizes or charges of the cations are rather different, the superstructure has a unit cell which is a few times larger

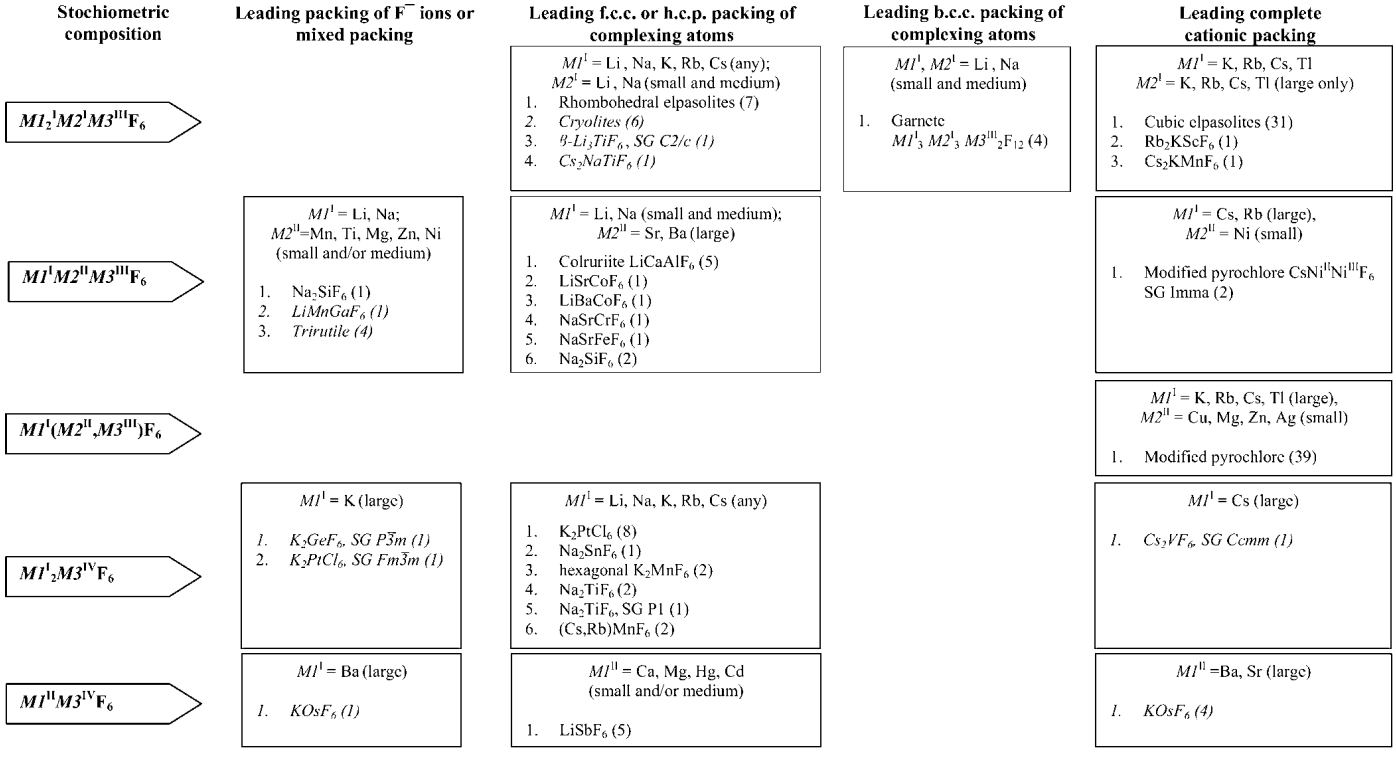

Figure 1
Classification of structure types of 3*d* metal complex fluorides by the chemical and stoichiometric composition of structure-forming sublattices. The number of compounds in each structure type is given in brackets after its name; compound names of 'intermediate' structure types are italicized (see text).

Table 2
Frequency and topological features of structure-forming ionic sublattices for the main structure types in a sample of 139 3*d* metal complex fluorides $M1_nM2_mM3F_6$.

Sublattice type	Number of compounds	Prototypes	Number of compounds in structure type	Topological features of sublattice
Anionic {F}	1	Na_2SiF_6	1	h.c.p.
Intermediate variant between leading sublattices {*M*3} *and* {F}	6	Trirutile	4	13, 49, 110
		$LiMnGaF_6$	1	F: h.c.p. *M*3(1): 14, 44, 104 *M*3(2): 11, 47, 98
		β-Li_3TiF_6	1	F: 9L packing *M*3(1): 14, 48, 108 *M*3(2): 13, 49, 106
Sublattice of complex ions or complexing atoms {*M*3}	43	K_2PtCl_6, Na_2SnF_6, (Cs,Rb)MnF_6, $LiSbF_6$, Na_3FeF_6, rhombohedral elpasolite	24	f.c.c.
		Colquiriite $LiCaAlF_6$, Na_2SiF_6, $NaSrCrF_6$, hexagonal K_2MnF_6, $NaSrFeF_6$, $LiSrCoF_6$, $LiBaCoF_6$	12	h.c.p.
		Fluorogarnet	4	b.c.c.
		Trigonal and triclinic Na_2TiF_6	3	F: h.c.p. *M*3(1): 14, 44, 104 *M*3(2): 11, 47, 98
Intermediate variant between leading sublattices {*M*3} *and* {*M*1,F}	2	hexagonal K_2MnF_6	1	*M*3: h.c.p. *M*1, F: 4L packing
		Rhombohedral elpasolite	1	*M*3: f.c.c. *M*1, F: 12L packing
Intermediate variant between leading sublattices {*M*3} *and* {*M*1,*M*2,*M*3}	6	Cryolites, distorted cubic elpasolite	6	*M*3: f.c.c. *M*1, *M*2, *M*3: b.c.c.
Complete cationic {*M*1,*M*2,*M*3}	74	Modified pyrochlore	41	*M*1: 16, 52, 130 *M*2, *M*3: 12, 50, 110
		Cubic elpasolite	33	b.c.c.
Intermediate variant between leading sublattices {*M*1,*M*2,*M*3} *and* {*M*1,F}	7	K_2GeF_6	1	*M*1, *M*3: b.c.c. *M*1, F: h.c.p.
		$KOsF_6$	5	*M*1, *M*3: b.c.c. *M*1, F: F: 13, 49, 113 *M*1: 14, 48, 116
		Cs_2VF_6	1	*M*1(1): 13, 50, 107 *M*1(2): 13, 48, 107 *M*3: 14, 48, 108 *M*1, F(1): 12, 45, 104 F(2): 11, 41, 100 F(3), *M1*(1): 13, 49, 102 *M*1(2): 13, 45, 104

than in the prototype (Wells, 1986). The crystal structures of the complex fluorides were also noted to be stabilized owing to the appropriate arrangement of cations over voids in the fluoride packing, *i.e.* because of the maximum isolation of cations of the same chemical type from each other (Babel, 1967; Wells, 1986; Sekino *et al.*, 1990).

Note that these regularities cannot unambiguously predict the crystal structures of structurally unexplored compounds. Thus, the aim of this study is to enlarge the list of such regularities or to improve them with the recently developed methods of crystallochemical analysis (Blatov, 2000, 2001).

2. Experimental

2.1. Investigated objects

The crystal data on 139 inorganic ternary and quaternary 3*d* metal complex fluorides were obtained from the Inorganic Crystal Structure Database (2001) using the program package

Table 3
Topological properties of ionic sublattices in the crystal structure of caesium hexafluoromanganate(IV) (Hoppe & Hofmann, 1977), belonging to the K_2PtCl_6 structure type, and corresponding values of the uniformity criterion G_3.

Sublattice type	Sublattice composition	Coordination sequence, $\{N_{1-3}\}$	G_3
Anionic	F^-	8, 30,68	0.0918
Cationic	Cs^+	6, 18, 38	0.0833
	Mn^{4+} (or $[MnF_6]^{2-}$)	12, 42, 92	0.0787
Complete cationic	Cs^+, Mn^{4+}	Cs: 10, 34, 82 Mn: 8, 36, 78	0.0862
Mixed cationic–anionic	Cs^+, F^-	12, 42, 92	0.0832
	Mn^{4+}, F^-	F: 5, 10, 37 Mn: 6, 24, 18	0.1006
Complete cationic–anionic	Cs^+, Mn^{4+}, F^-	Cs: 12, 34, 112 Mn: 6, 32, 66 F: 9, 38, 81	0.0857

TOPOS (Blatov *et al.*, 2000) for multipurpose crystallochemical analysis. The compounds belong to 33 structure types; the most frequent structure types are Na_2SiF_6, trirutile, colquiriite, cubic K_2PtCl_6, rhombohedral and cubic elpasolites, hexagonal K_2MnF_6, fluorogarnets, cryolites, modified pyrochlore, $KOsF_6$ and $LiSbF_6$ (Tables 1 and 2). The sample included the crystal structures of fluorides that were completely determined, with $R_f \leq 5\%$. A topological model of the crystal structure was built for each compound using the programs *AutoCN*, *ADS* and *IsoTest* of the *TOPOS* package, and analysed with the methods described below.

2.2. Definition of structure-forming sublattice

Let us consider the ionic crystal as a system of charged spherical particles. As the electrostatic energy of such a system is an additive value, one can arbitrarily group the terms in the sum

$$E_{\rm ion} = \tfrac{1}{2}\sum_i E_i, \qquad (1)$$

where E_i is the energy of the electrostatic interaction of an ith atomic pair; each variant of such a grouping corresponding to a *model* of crystal structure. In this study we will analyse the decomposition

$$E_{\rm ion} = E_{\rm cc} + E_{\rm aa} + E_{\rm ca}, \qquad (2)$$

where $E_{\rm cc}$ and $E_{\rm aa}$ are the energies of electrostatic repulsion between cations and anions, respectively, and E_{ca} is the energy of cation–anion attraction. In addition, if crystal structures contain chemically different ions, each term in (2) should contain several components; several competitive models must be considered in this case. For instance, the crystal structure of Cs_2MnF_6 (Hoppe & Hofmann, 1977) can be represented with at least three models:

(i) The packing of fluoride ions with the Mn^{4+} and Cs^+ cations allocated in the packing voids.

(ii) Mixed f.c.c. (face-centred cubic) packing of F^- and Cs^+ ions with the Mn^{4+} ions arranged over octahedral F_6 voids.

(iii) F.c.c. packing of $[Mn^{IV}F_6]^{2-}$ complex ions with the Cs^+ cations in the voids.

Note that in most of the structure investigations authors only consider the features of the coordination sphere for cations (*i.e.* take into account only first terms in $E_{\rm ca}$) and use the models relating to $E_{\rm cc}$ and $E_{\rm aa}$ terms much less frequently. At the same time, the uniform arrangement of like-charged ions should reduce the two terms in (2) and $E_{\rm ion}$ as a whole. Thus, estimating the degree of uniformity of various ionic sublattices in a crystal structure one can find the sublattice, which make the greatest contribution to stabilization of the crystal structure compared with other sublattices. It is the most uniform sublattice that may be considered as *structure-forming* (or *leading*; Blatov, 2001; Peresypkina & Blatov, 2002), because it provides the stability of the whole crystal structure. Note that the well known tendencies of like cations were to be isolated as much as possible and their environment to be distorted (Babel, 1967; Massa & Babel, 1988), which leads to the realisation of typical coordination numbers, following the preference of separate ionic sublattices for a uniform (or locally uniform) spatial arrangement. Similar ideas were stated by Borisov & Podberezskaya (1984) and Borisov (2000) for ionic frameworks as structure-forming motifs in binary inorganic fluorides, sulfides and oxides with heavy cations. Borisov (2000) showed that structure-forming matrices in these crystal structures included heavy cations and the number of matrices was limited; they were f.c.c. and b.c.c. (body-centred cubic) lattices, as a rule. Recently, the ideas concerning the essential structural importance of cationic motifs in structure formation were developed by O'Keeffe & Hyde (1985), Vegas *et al.* (1991) and Vegas & Jansen (2002).

In this connection it is important to distinguish the notions 'packing' and 'structure-forming sublattice', since the structure-forming sublattice is generally not a packing, *i.e.* the constituent ions are not necessarily in contact. The packing of contacting ions always forms a framework, which is the basis of the crystal structure, and it can be stabilized by interactions between other ions to constitute the structure-forming sublattice in this case. In the crystal structures of complex fluorides with the fluoride ions having a clear structure-forming role, the structure-forming sublattices are also packings. However, if the complete cationic sublattice plays the leading role, the packing consists of fluoride ions or similar-sized cations and anions, as, for instance, fluoride ions and some alkali cations in the ordered perovskites. The same structure type may occur for differently distorted crystal structures that may highlight the different structure-forming roles of one-type sublattices, as, for instance, for Cs_2MnF_6 (Table 3) compared with other compounds of the K_2PtCl_6 type (Table 1). If compounds belonging to the same structure type are distorted they may be characterized by different models. Therefore, while searching for a structure-forming sublattice one needs to estimate to which degree the crystal structures and their components are distorted even within the same structure type.

2.3. Uniformity criterion for atomic sublattices and search for the most uniform ionic sublattices

To measure the distortion degree of a lattice Blatov (2001) proposed the parameter of lattice uniformity to be the mean-square error of the lattice quantizer:

$$G_3 = \frac{1}{3}\left[\frac{1}{Z}\sum_{i=1}^{Z}\int_{\mathrm{VDP}(i)} R^2 \mathrm{d}V_{\mathrm{VDP}(i)}\right] \Big/ \left\{\frac{1}{Z}\sum_{i=1}^{Z} V_{\mathrm{VDP}(i)}\right\}^{5/3}, \quad (3)$$

where Z is the number of atoms in the asymmetric unit, $V_{\mathrm{VDP(i)}}$ is the volume of Voronoi–Dirichlet polyhedron of an ith atom and R is the distance between the ith atom and some interior point of its Voronoi–Dirichlet polyhedron. The quantizer is generally a multilattice embedded into crystal space. When applied to the compounds considered, each quantizer node coincides with the position of a structural unit (for example, monatomic or complex ion). Such a simplified representation of crystal structure allows one to determine the G_3 parameter for any atomic (ionic) sublattice; the smaller the G_3 value the more regular the spatial atomic (ionic) arrangement in the sublattice. Note that among periodic lattices the smallest value is $G_3 = 0.07854$, which corresponds to the b.c.c. lattice, while $G_3 = 0.07875$ characterizes close packing (Convay & Sloane, 1988). To correctly analyse the data obtained it is important to keep in mind that the error of G_3 estimated from experimental data is ~ 0.0005. Thus, a pair of G_3 values is equal, within error, when $\Delta G_3 = |G_3(1) - G_3(2)| \leq 0.001$, where the 1 and 2 indices correspond to different atomic sublattices (Peresypkina & Blatov, 2002).

Let us emphasize that the G_3 parameter estimates the uniformity of the spatial arrangement of *points* (for instance, point charges). To estimate the uniformity of the spatial arrangement of spheres using (3), integration should only be performed over the part of the Voronoi–Dirichlet polyhedron that is outside the sphere in the atom. In this case, the arrangement with minimum G_3 should correspond to the maximum intersection of the spheres with Voronoi–Dirichlet polyhedra. It is the close packing that obeys this condition and it is the most uniform arrangement of spheres (not points).

2.4. Method for topological analysis of atomic sublattices

In addition to the quantitative criterion for the distortion degree of ionic sublattices, we have used the method using the unambiguous description of sublattice topology. This method is based on the representation of a crystal structure as a graph, whose nodes symbolize atoms and edges connecting the nodes imitate the different types of chemical bonds between pairs of atoms (Blatov & Serezhkin, 2000). Although such a *complete* graph of crystal structure allows one to extract data from bond lengths and angles, it cannot practically clarify the role of each type of atom whilst the crystal structure is forming. Therefore, in the framework of the topological description several alternative models can be proposed to represent the crystal structure by graphs of separate sublattices $\{A1, A2, \ldots\}$ to be composed of the atoms $A1, A2, \ldots$ of one or several chemical sorts. To select a subset of atoms, corresponding to a sublattice of atoms, ions or other structural units, one should construct an '*incomplete*' graph (Blatov, 2000) or *packing graph* (Blatov, 2001), whose connectedness can be restored with the Voronoi–Dirichlet partition. Namely, if an atomic pair shares a rather large face of the Voronoi–Dirichlet polyhedron [solid angle of the face $\Omega \geq 1$–1.5% of 4π steradian (Blatov, 2001)], the corresponding edge appears in the packing graph. According to Blatov (2000), one can separate N_t, different atomic sublattices, depending on the number of different chemical types (m) of atoms in the crystal structure

$$N_t = \sum_{l=1}^{m}\{m!/[l!(m-l)!]\}. \quad (4)$$

For instance, $N_t = 7$ and 15 for ternary and quaternary compounds, respectively, but atomic sublattices are not all of interest in the context of crystallochemical analysis. The sublattices to be selected depend on the concrete problem to be solved (Blatov, 2000). Therefore, we will restrict our study by detailed analysis of anionic, complete cationic and complexing atom sublattices (Tables 1 and 2). Mixed cationic–anionic sublattices are only taken into account if they correspond to close packings. Thus, in terms of the method described, the well known models of the crystal structure Cs_2MnF_6, listed in §2.2, can be represented as:

(i) The sublattices {F}, {Cs} and {Mn}. The connectedness of each sublattice should be restored using the Voronoi–Dirichlet partition for the corresponding ionic array.

(ii) The sublattices {F, Cs} and {Mn}.

(iii) The sublattices {Cs} and {Mn}; the F atoms are out of consideration in this case, *i.e.* the complex position can only be determined with the complexing atom.

To investigate the topological properties of sublattices we have used the method of coordination sequences proposed by Brunner & Laves (1971) and applied for both organic (Peresypkina & Blatov, 2000*a*) and inorganic (Blatov, 2001; Blatov & Zakutkin, 2002; Peresypkina & Blatov, 2002) crystal structures. The method provides an accurate count of the number of graph nodes in the coordination spheres of a given node, starting from the first sphere ($k = 1$) and then ($k = 2, 3, \ldots, n$) up to the nth sphere. The set of integers $\{N_k\}$ ($k = 1 - n$) forms the coordination sequence, which obeys analytical quadratic equations (O'Keeffe, 1995). If $\{N_k\}$ sets are different for a pair of sublattices the sublattices are strictly non-isomorphic, otherwise one can assume that they are topologically identical within the first n coordination spheres. Thus, equal $\{N_k\}$ sets mean no strict isomorphism of compared graphs, however, the greater the k value the more similar the topological properties of compared sublattices. In this study, following Peresypkina & Blatov (2000*a*) and Peresypkina & Blatov (2002), we have analysed the coordination sequences for sublattices within the first three coordination spheres to identify their *essential* isomorphism (Blatov, 2000).

2.5. How to determine the structure-forming role of packing and sublattices

As mentioned above, to quantitatively prove the leading role of a sublattice its geometrical uniformity criterion value G_3 can be used. For this purpose one should compare G_3 values for all the ionic sublattices and select the sublattice with the minimum G_3 value. For example, in the crystal structure of Cs_2MnF_6 (Table 3) the structure-forming sublattice consists of complexing atoms (centres of complex ions $[Mn^{IV}F_6]^{2-}$) and its G_3 value is typical for ideal f.c.c. lattices (Blatov, 2001). According to Table 3, the only variant corresponding to the f.c.c. packing of $[Mn^{IV}F_6]^{2-}$ complex ions with countercations in the voids should be selected out of different models of the Cs_2MnF_6 crystal structure (§2.2), which seems chemically reasonable. Moreover, not only the minimum value of the uniformity criterion of the sublattices needs to be considered, but also their topological properties as well, which are characterized by the $\{N_k\}$ set.

(i) If a sublattice of monatomic ions may be considered as a packing in the context of the model accepted, the ideal G_3 value for the sublattice is 0.07875..., and the most efficient motif is the close packing, corresponding to the most uniform arrangement of hard spheres. If a sublattice consists of multiatomic ions, the G_3 value can deviate from the ideal value owing to their non-spherical shape.

(ii) If the ions do not contact each other in a sublattice and therefore can be considered as point charges, the ideal G_3 value for the sublattice is 0.07854 and the most efficient motif is the b.c.c. lattice, corresponding to the most uniform arrangement of points.

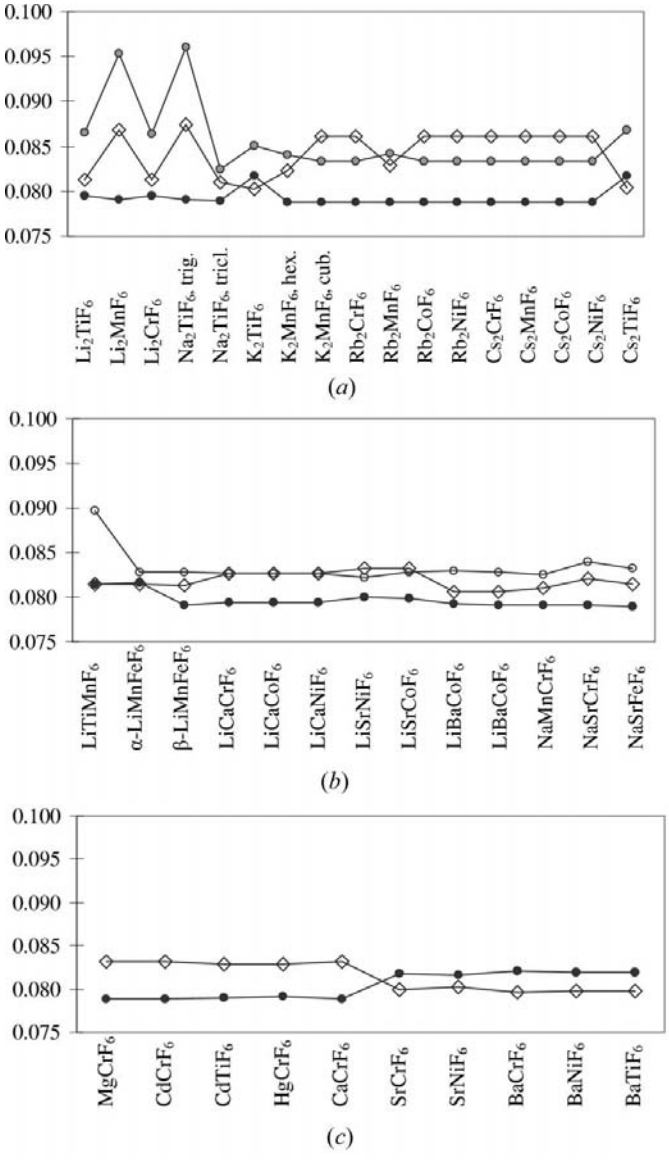

Figure 2
Change in G_3 values in the series (*a*) $M1^{I}{}_2M3F_6$, (*b*) $M1^{I}M2^{II}M3F_6$ and (*c*) $M1^{II}M3F_6$. In each series the compounds are arranged in ascending order of the countercation radii. G_3 values for the complete cationic sublattice are shown by rhombs; circles correspond to G_3 values for the sublattices $M3^{III,\,IV}$ (black), $M1^{I}$ (grey) and $\{M3^{I}, M2^{II}\}$ (white). In (*c*) G_3 values of the sublattices $M1^{II}$ and $M3^{IV}$ are equal.

3. Results

The classification scheme for 139 inorganic complex fluorides of the first transition series (Fig. 1) shows a direct relationship between structure-type features and the chemical composition of compounds. The analysis of G_3 values allows detection of the common types of leading ionic sublattices (Table 2, Fig. 1):

(i) Anionic sublattice that corresponds to the packing of the fluoride ions.

(ii) Complete cationic sublattice, corresponding to the sublattice of cations.

(iii) Sublattice of complexing atoms, corresponding to the packing of complex ions.

(iv) Intermediate variants.

As a result the fluorides can be classified into three main groups (Fig. 1):

(i) Complex fluorides based on the leading packing of monatomic ions: This group includes nine polymorphs of complex fluorides, belonging to six structure types, namely trirutile, Na_2SiF_6 and $LiMnGaF_6$, closely related to Na_2SiF_6, which are based on the packings of fluoride ions, and K_2TiF_6, K_2PtCl_6 and $KOsF_6$ types comprising mixed packings of fluoride ions together with countercations. Note that all these compounds contain small and/or medium cations $M1^{I}$ (Li, Na) and $M2^{II}$ (Ti, Fe) in $M3^{III}$ derivatives or cations of any size in the case of $M3^{IV}$ fluorides. Three compounds are based on h.c.p. packing and one fluoride has f.c.c. packing of structure-forming ions.

(ii) Complex fluorides based on the leading complete cationic sublattice: This group of 79 compounds consists of seven structure types, namely $KOsF_6$, cubic and trigonally distorted elpasolites, modified pyrochlore and related superstructures (Fig. 1). Motifs of cationic sublattices correspond to b.c.c. for 37 compounds and to the crystal structure of the Laves phase $MgCu_2$ for 41 compounds. Only in the case of Cs_2VF_6 is the cationic sublattice essentially distorted and unrelated to frequent sublattice types. All these compounds contain at least one type of large countercation; the elpasolite

Table 4
Changes in G_3 uniformity criterion for ionic sublattices in the crystal structure of Rb_2KScF_6 elpasolite (Flerov *et al.*, 2002) at thermal polymorphism.

Particular topological properties are shown in brackets; G_3 values for ideally uniform sublattices are italicized.

Sublattice composition and type	G_3 values		
	$P2_1/n$, T = 150 K	$I4/m$, T = 240 K	$Fm\bar{3}m$, T = 300 K
Rb^I, F^- (f.c.c.)	0.0814	0.0810	0.0809
K^I (f.c.c.)	*0.0788*	*0.0788*	*0.0788*
Sc^{III} (f.c.c.)	*0.0788*	*0.0788*	*0.0788*
Rb^I, K^I, Sc^{III} (b.c.c.)	0.0786	*0.0785*	*0.0785*
F^-	0.0865	0.0886	0.0892

Table 5
Changes in G_3 values for ionic sublattices in the crystal structure of Cs_2NaTiF_6 elpasolite (Alter & Hoppe, 1989; Becker & Hoppe, 1974) with thermal polymorphism.

See footnotes to Table 4.

Sublattice composition and type	G_3 for Cs_2NaTiF_6 phase	
	$R\bar{3}m$, LT	$P\bar{3}m1$, HT
Cs^I, F^-	0.0810 (12 L)†	0.0800 (6 L) †
Na^I	0.0820	0.0795 (f.c.c.)
Ti^{III} (f.c.c.)	*0.0788*	*0.0788*
Cs^I, Na^I, Ti^{III}	0.0802	0.0796
F^-	0.0909	0.0896

† Multi-layered close packing.

crystal structures comprise only large countercations; Cs_2NaMnF_6 and Cs_2NaFeF_6 are exceptions and belong instead to fluorides with the structure-forming role of complex ions (see Fig. 1). The crystal structures of $M1_2M2M3F_6$ fluorides are based on mixed cationic–anionic packings; $M3^{III}$ derivatives and other $M3^{IV}$ derivatives are constructed with rather distorted anionic packing.

(iii) Complex fluorides with the leading sublattice of complex ions [$M3^{III,\ IV}F_6$] (Fig. 1): It is important that this sublattice always has f.c.c., h.c.p. (hexagonal close packing) or b.c.c. topology. There are 51 complex fluorides out of 23 structure types in this group. Cubic K_2PtCl_6, rhombohedral elpasolite, cryolite, garnet, hexagonal K_2MnF_6, $LiSbF_6$, Na_2SiF_6 and colquiriite $LiCaAlF_6$ structure types are the most frequent (Fig. 1, Table 1). Several structure types, β-Li_3TiF_6, Cs_2VF_6, Cs_2NaTiF_6 and typical cryolites, have at least one more highly uniform sublattice in addition to the sublattice of complexing atoms; they are included in this group because of the slightly higher uniformity in the latter one. We have found no clear correlation between structural features and chemical composition in this group. However, $M3^{III}$ derivatives often contain large countercations, such as $M1^I$ = K, Rb, Cs, in combination with small and medium countercations $M2^I$ = Li, Na. At the same time the $M3^{IV}$ derivatives comprise any $M1^I$ ions and only small $M1^{II}$ = Mg, Ca, Cd, Hg countercations.

Note that the classification of some compounds was relative when the sublattices to be compared are equiuniform, *i.e.* when $\Delta G_3 \leq 0.001$. To avoid this problem the topological properties of sublattices should be taken into account. In this case, even a little higher distorted sublattice should play a leading role if it has the topology of a sublattice that can be highly uniform (*i.e.* f.c.c. or b.c.c.). It was the reason for choosing 21 *intermediate* complex fluorides belonging to nine structure types (Table 2). Their crystal structures will be discussed separately in §4.4. To simplify the scheme (Fig. 1), all 'intermediate' compounds are put into the main groups of compounds according to the most uniform sublattices formally, but are italicized.

4. Discussion

4.1. Structure-forming packing of monatomic ions

Complex ions (alternatively *M*3 cations) have weak structure-forming roles in fluorides of this group; the leading role belongs either to the packing of fluoride ions or to the sublattice of cations (Table 2). This is the reason why the compounds are considered as close packings of fluoride ions with *M*1, *M*2 and *M3* cations, partially occupying tetragonal and/or octahedral voids (Babel, 1967; Courbion *et al.*, 1982; Sekino *et al.*, 1990) or as mixed cationic–anionic packings if the size of the F ion and one of the countercations is similar (Babel, 1967; Wells, 1986). Both packings are somewhat distorted by the metal ions allocated in voids. Note that even the lithium ion [with minimum $r \simeq 0.68$ Å (Wells, 1986)] should distort the ideal initial geometry of the packing when allocated to its octahedral void. Therefore, the anionic (or mixed) sublattice is not usually the most uniform, but only keeps the h.c.p. topological motif.

4.1.1. Structure-forming packing of fluoride ions. There is only the compound α-$LiMnFeF_6$ (Courbion *et al.*, 1982) of the Na_2SiF_6 type to be stabilized owing to fluoride packing, which is definitely more uniform than the complete cationic sublattice (ΔG_3 = 0.0020). However, despite the small sizes of cations, structure-forming fluoride packing is somewhat distorted (G_3 = 0.0794). Besides, in the high-temperature β-$LiMnFeF_6$ phase, the packing increases its distortion and loses its strongly marked structure-forming role, but keeps the h.c.p. topological motif. Obviously, medium and large cations will cause greater distortions still in the packing of fluoride ions (Table 1). Note that the crystal structures of complex fluorides are often described in the literature as packings of fluoride ions with small cations in the voids. However, in most cases significant distortions (Table 1) are the evidence of a feebly marked structure-forming role of such packing. At the same time the cationic sublattices responsible for the distortions remain rather uniform (Table 1). This is the reason to place the remaining five fluorides belonging to trirutile and $LiMnGaF_6$ types into this group. Formally the fluoride packing has a minimum G_3 value, but in fact these compounds contain high uniform cationic sublattices, which are in competition for the structure-forming role with fluoride packings (§4.4).

4.1.2. Mixed structure-forming packing. There is no fluoride with a marked structure-forming role of mixed packing. However, in the crystal structures of the nine inter-

mediate compounds mixed sublattices are among the most uniform ones (Table 3) and they share their leading role either with complete cationic sublattices (in the crystal structures of Cs_2VF_6, K_2TiF_6 and five compounds of the $KOsF_6$ structure type) or with the sublattices of *M*3 cations (in the crystal structures of cubic K_2MnF_6 and elpasolite Cs_2NaTiF_6). These compounds will be considered in detail in §§4.4 and 4.5.3.

4.2. Structure-forming sublattice of complexing atoms

Compounds of this group in which the structure-forming role of the *M*3 sublattice is marked allow an ambiguous choice of structure model. On the one hand, the *M*3 atom is the centroid of the complex and since the $[M3F_6]$ sublattice is also a packing, the complex fluorides can be considered as $[M3F_6]$ packings with *M*1 and *M*2 countercations in the packing voids. On the other hand, the highly uniform arrangement of *M*3 cations may be caused by the preference of any highly charged cation to be isolated. In this case the crystal structure should be considered as a packing of monatomic ions (anionic or mixed), where *M*3 cations occupy anionic voids. It is difficult to prefer one of the alternative models. Nevertheless, the calculation of the G_3 criterion shows that irrespective of the nature of the structure-forming lattice, except completely cationic lattices, the *M*3 sublattice is the most uniform among various cationic sublattices for most of the fluorides (§4.5.2). In our opinion, this fact is evidence of the preference of highly charged cations to be isolated or, in other words, to be arranged uniformly. Note that the only way to verify one of these models is to study non-symmetric complexes with different ligands, where the positions of the complex centroid and the complexing atom are far apart.

As mentioned above, in this group of compounds the *M*3 sublattices always have topological features of f.c.c., h.c.p. (much rarer than other close packings) or b.c.c. lattices (Tables 1 and 2), which is in good agreement with the concept of Borisov (2000) and with two ambiguous models showing the structure-forming role of *M*3 cations. Note that in 53% of compounds these packings are non-distorted and in the remaining compounds the distortions are insignificant. The most significant distortion is found for h.c.p. in the crystal structure of $LiSrNiF_6$ (the colquiriite structure type, Table 1), where $G_3(Ni^{III}) = 0.0799$ and only about 1.5% greater than the G_3 value for ideal close packing (Blatov, 2000).

The analysis of chemical composition shows that the structure-forming role of complexes becomes stronger if:

(i) countercations are medium or large and small cations are combined in some ratio, and

(ii) they occupy most of the packing voids.

Thus, if only one third of the voids (two tetrahedral and one octahedral) falling to the complex anion are occupied in an $[M3F_6]$ packing, the structure-forming role of the packing is unlikely because such a structure model conflicts with the principle of maximal space filling (Vainshtein *et al.*, 1983). In this case the packing of fluoride ions is more likely to occur, which is distorted by the cations uniformly occupying the voids. This fact is indirectly confirmed by the lack of $M1M3F_6$ fluorides with the marked leading role of the complex ions (Tables 1 and 2). Thus, in the crystal structures of nine $M1M3F_6$ fluorides, $\Delta G_3 = |G_3(F^-) - G_3(M3)| = 0.0014$–$0.0024$ and only the $CdTiF_6$ crystal has a higher ΔG_3 value (0.0030) and a stronger marked leading role of the complex ions. Since the cations $M2^{II}$ = Ti, Mn, Cd, Ca and $M3^{IV}$ are small, fluoride ions can play a structure-forming role within the $LiSbF_6$ structure type, especially because they form an h.c.p. packing in all these compounds. Clearer conclusions can likely be made after studying the polymorphism of these compounds.

If countercations occupy two thirds of the voids in an $[M3F_6]$ packing, the complexes in most cases play the leading role whilst forming the crystal structure. However, this statement is correct only for large cations in $M1M2M3F_6$ fluorides, namely for $M2^{II}$ = Ba, Sr and for any $M1^{I}$ cations in $M1_2M3F_6$ fluorides (Fig. 1). If all voids are occupied in an $[M1F_6]$ packing, as in the crystal structures of $M1_2M2M3F_6$ fluorides (cryolites and rhombohedral elpasolites), the countercations can have any size, but cannot all be large, since such a combination should destabilize the crystal structure (Massa & Babel, 1988; Flerov *et al.*, 1998). If countercations $M1^{I}$ and $M2^{I}$ are large, the $M1_2M2M3F_6$ fluorides have another crystal structure of cubic (instead of rhombohedral of hexagonal) elpasolite and another structure-forming component, namely a complete cationic sublattice (Table 1, Fig. 1). Note that it is the elpasolite family where polymorphs exist with both rhombohedral and cubic crystal structures. These compounds comprise one small and two large countercations (for instance, α- and γ-polymorphs of Cs_2NaMnF_6 and Cs_2NaFeF_6; Massa, 1982; Herdtweck *et al.*, 1986; Babel & Haegele, 1976); obviously, they are 'intermediate' between the structure types based on the leading sublattice of complex ions and on the cationic framework. This fact will be discussed in §§4.4.4 and 4.5.3. One more high-pressure phase, Li_2CrF_6, will also be considered in §4.5.3.

4.3. Structure-forming cationic sublattice

As was mentioned above, cations tend to be arranged as uniformly as possible in the space available; the larger the cation the stronger the tendency. The topologies of their complete sublattices depend on the size of the countercation. For example, large cations prefer the b.c.c. lattices of all the possible arrangements, which is ideal in most cases. This feature is not surprising; as was mentioned above, the most uniform variant of an arrangement for non-contacting ions of the same charge is a b.c.c. lattice. Whilst allocating in voids, the large cations distort the close packing; the motif of close packing is unstable and should not appear. The stability of the crystal structure then depends on the energetic stability of the spatial arrangement formed by large cations. Therefore, the size of the cation is the factor increasing its structure-forming capability (§4.5.1). Thus, when large cations occupy the voids of the fluoride packing, the structure-forming roles of cationic and anionic sublattices are equalized or the structure-forming component is changed. In modified pyrochlore crystal structures constituent cations are both large and small. Besides this,

Table 6
Predicting structural features of $M1_nM2_mM3F_6$ 3*d* metal complex fluorides depending on the correlation between charges (z), radii (r) and the stoichiometric ratio of ions.

'Intermediate' types (Table 2) were not taken into account when making up the scheme; the ionic radii are arranged in descending order $r(M1) \geq r(M2) \geq r(M3)$; ionic charges are arranged in ascending order $z(M1) \leq z(M2) \leq z(M3)$.

Structure feature	Condition I	Result	Condition II	Result	Conclusion
Composition of the packing	$r(M1)$, $r(M2) \simeq r(F)$	Yes	–	–	Cationic–anionic
		No	–	–	Anionic
Topology of the packing	$r(M1) << r(F)$	Yes	–	–	Close packing
		No	–	–	Distorted
Topology of cationic sublattice	$r(M1) \simeq r(M2) >> r(F)$	Yes	$6/(n+m+1) < 2/3$	No	B.c.c. for {*M*1, *M*2, *M*3}
				Yes	F.c.c. or h.c.p. for {*M*3}
		No	$r(M1) >> r(F)$	No	
			$r(M1) >> r(M2)$, $z(M1) < z(M2) < z(M3)$		
				Yes	Topology of the Laves phase $MgCu_2$ for {*M*1,*M*2,*M*3}

their charges are different and the cationic array has the topology of the Laves phase $MgCu_2$ (Table 2; Ohba *et al.*, 1984). In this case the cationic sublattices are also rather uniform and are characterized by $G_3 = 0.0793$ for all cubic modified pyrochlores and only slightly less uniform ($G_3 = 0.0800$) for ordered modified pyrochlores $M1^{I}Ni^{II}Ni^{III}F_6$, $M1^{I}$ = Cs, Rb (Table 1). Obviously, the cations with different size and charge should prefer this type of arrangement because of the local uniformity and energetic stability which allows them to reach different coordination numbers; namely, $N_1(M1) = 16$, $N_1(M2) = 12$ (Frank & Kasper, 1958). Note that the cationic structure-forming sublattices are significantly more uniform than fluoride or the cationic–anionic structure-forming packings.

Although the cationic sublattice stabilizes the crystal structure, it is not a packing itself, therefore, various types of packings can occur in such crystal structures. Thus, ionic packings in the crystal structures of $M1_2M2M3^{III}F_6$ fluorides are often mixed (cationic and anionic) since these compounds, as a rule, contain similar-sized $M1^{I}$ cations and anions. Strongly distorted anionic packings are realised in the crystal structures of $M1M2M3^{III}F_6$ and $M3^{IV}$ fluorides. The aforementioned high-pressure phases of Cs_2NaMnF_6 and Cs_2NaFeF_6 are exceptions.

4.4. 'Intermediate' crystal structures

In a number of complex fluorides it is impossible to detect a single structure-forming lattice, as G_3 values of two (or more) ionic sublattices are equal within the error of the G_3 calculation. Moreover, for all 21 'intermediate' compounds equiuniform sublattices with a high structure-forming role relate to different models. In terms of graph theory, this indicates an intersection of the atomic sets which make up the 'incomplete' graphs. Exceptions can only be found for the 'intermediate' compounds, where one of the most uniform sublattices is the sublattice of complexing atoms that allows the aforementioned alternatives while constructing the structure model. Thus, the 'intermediate' compounds are stabilized by several highly uniform sublattices. Let us consider all the variants of such combinations.

4.4.1. Fluoride packing and the sublattice of complexing atoms. This variant of the combination of structure-forming sublattices occurs in the crystal structures of six 'intermediate' fluorides, belonging to the $LiMnGaF_6$, trirutile and β-Li_3TiF_6 structure types. According to Courbion *et al.* (1982), in the crystal structure of β-$LiMnFeF_6$ ($LiMnGaF_6$ type), as with the α-phase, the fluoride sublattice has an h.c.p. motif caused by the small size and weak structure-forming capability of the cations. When occupying the voids of close fluoride packing these cations not only distort the packing, but also keep its topological motif (Babel, 1967; Courbion *et al.*, 1982). In the crystal structures of four fluorides related to the trirutile type (Table 1) the anionic packing is the most uniform, but distorted. Thus, the h.c.p. anionic motif of the rutile type disappears. The distortion yields packing close to the b.c.c. lattice according to the criterion of Blatov (2001): the values $N_{1-3} = \{13, 49, 110\}$ are close to b.c.c. $N_{1-3} = \{14, 50, 110\}$ (Table 1). In the β-Li_3TiF_6 crystal structure the sublattice of the *M*3 cations and the nine-layered close packing of the fluoride ions are the most uniform (Tables 1 and 2). The compromise between these two sublattices is caused by the weak structure-forming capability and the small size of the lithium cations. This feature allows the slightly distorted ($G_3 = 0.0794$) packing of fluoride ions to appear along with the rather uniform motif of highly charged *M*3 cations. Besides, this is a high-temperature phase that also encourages complexing atoms to have a uniform arrangement (§4.5.3). As a result the compromise variant occurs with the leading role of the fluoride ions, whose sublattice keeps the close-packing topology (Table 1).

4.4.2. Mixed cationic–anionic packing and the sublattice of complexing atoms. In two 'intermediate' fluorides, namely cubic K_2MnF_6 (the K_2PtCl_6 type) and Cs_2NaCoF_6 (cubic elpasolite), the structure-forming roles of the mixed cationic–anionic packing and the sublattice of complexing atoms are almost the same. Other compounds of these structure types are not 'intermediate' and are based on the packing of complexes and on the complete cationic sublattice, respectively. In our opinion, this example shows that structure types can be stabilized in two ways: by selecting either the single most uniform sublattice or several equiuniform sublattices

simultaneously. This is likely the reason why these structure types are so widespread. Note that the same properties are characteristic of the Na_2SiF_6, $KOsF_6$ and cryolite structure types, whose structure organization allows compounds with various combinations of structure-forming sublattices to exist (Table 2). In these structure types G_3 values for atomic sublattices vary over a wide range (Table 1).

4.4.3. Mixed cationic–anionic packing and the complete cationic sublattice. This group, which is one of the largest groups of 'intermediate' fluorides, includes seven $M1^{I}_{2}M3F_6$ and $M1^{II}M3F_6$ fluorides, which can be described in terms of two different models based on the complete cationic sublattice or mixed cationic–anionic packing (Table 2). All compounds of the group comprise large $M1^{I}$ = K, Cs and $M1^{II}$ = Ba, Sr countercations that yield mixed packings. Five fluorides are based on a b.c.c. complete cationic sublattice, which indicates the cations to be structure-forming components despite the sublattice distortion. Only two compounds with the $M1^{I}_{2}M3F_6$ composition are intermediate between the h.c.p. mixed packing of fluoride and potassium ions and the b.c.c. complete cationic sublattice: K_2TiF_6 (the K_2GeF_6 type) and Cs_2VF_6. In the K_2TiF_6 crystal structure the complete cationic sublattice is only slightly less uniform [$\Delta G_3 = G_3(K,F) - G_3(K,Ti) = 0.0009$], which separates K_2TiF_6 from other compounds with similar composition. Most belong to the K_2PtCl_6 structure type, where the cationic sublattice is structure-forming (Table 1). Similar regularities also are valid for Cs_2VF_6, however, in this case no special topology is found for structure-forming sublattices.

4.4.4. Sublattice of complexing atoms and the complete cationic sublattice. The last group of 'intermediate' structures consists of six compounds based on the complete cationic sublattice and the sublattice of complexing atoms, both with equally marked structure-forming roles: five cryolites and Cs_2NaTiF_6 trigonal elpasolite (Table 1). The cryolite family is of special interest as it includes six compounds belonging to two structure types: to cryolite Na_3AlF_6 itself and distorted cryolite Na_3FeF_6 (space group $P2_1$). In five of the six cryolites the models with the leading role of the cationic sublattice or the complex ions tend to compromise because the structure-forming capabilities of both the cationic sublattices and the complex ions are similar. For scandium, manganese and vanadium cryolites the value $\Delta G_3 = |G_3(M1,M2,M3) - G_3(M3)|$ varies in the range 0.0002–0.0005 and is comparable with $\sigma(G_3)$. Neither the b.c.c. cationic sublattice nor the f.c.c. packing of complex ions have the highest uniformity which is allowed by their topology. Despite the Jahn–Teller effect in the Na_3MnF_6 crystal structure, this compound does not fall out of the cryolite series because, according to Englich & Massa (1992), it is the compound with the least Jahn–Teller distortion of all the Mn^{III} derivatives. In the distorted crystal structure of iron cryolite the value $\Delta G_3 = 0.0011$ provides evidence of the higher leading role of the complex ions. Note that in the high-pressure crystal structure of scandium cryolite (Carlson *et al.*, 1998) the cationic sublattice is less uniform than at normal pressure. This fact allows discussion on the high stability of the structure-forming sublattice of complex ions, at least up to 68.2 kbar. Obviously, this stability is caused by the low structure-forming capability of sodium cations. In the high-temperature phase of Cs_2NaTiF_6 both the sublattice of the $M3$ ions and the complete cationic sublattice are highly uniform; this crystal structure will be discussed in detail in §4.5.3.

4.5. What factors influence the structure-forming role of the cationic sublattice?

4.5.1. Cation size. As mentioned above, in the morphotropic series of complex fluorides the reason for the increasing structure-forming capability of cations is the increase in their sizes. For instance, in the morphotropic series of nine $LiM2M3^{III}F_6$ compounds, the trirutile structure type, characteristic for three fluorides $(Li,M2)CoF_6$, $M2^{II}$ = Mg, Ni, Zn, changes to the colquiriite structure type ($LiCaM3F_6$, $M3^{III}$ = Cr, Co, Ni) and then to the $LiCdCoF_6$ and $LiBaCoF_6$ structure types (Viebahn, 1971). Let us interpret these transitions in terms of the changing structure-forming role of various structural components. The first compounds in the series, $(Li,M2)CoF_6$, are based on the most uniform fluoride packing. The substitution of Mg, Ni or Zn by the rather larger Ca causes distortions in the fluoride close packing and the simultaneous increase of the structure-forming capability of complex ions. In other words, the Ca cations equalize the leading roles of the sublattices. For instance, $G_3([Co^{III}F_6]) = 0.0794$ and $G_3(F^-) = 0.0809$ in the $LiBaCoF_6$ crystal structure. It is typical that an increase in the structure-forming role of $M2^{II}$ cations orders the $M1^{I}$ and $M2^{II}$ cations and results in superstructures. With increasing cationic size ($M2^{II}$ = Sr, Ba) the distortions in the fluoride packing become too large to keep the close-packing motif. For instance, $G_3([Co^{III}F_6]) = 0.0792$ and $G_3(F^-) = 0.0853$ in the $LiBaCoF_6$ crystal structure. Thus, the complex ions become the only leading component in these fluorides (Fig. 1) and the colquiriite structure type, where the leading role of the complex ions is not too marked, becomes unstable. For instance, the stability of the $LiSbF_6$ and $KOsF_6$ structure types, derived from NaCl and CsCl, respectively (Kemmitt *et al.*, 1963; Babel, 1967), can be explained for ten $M1M3^{IV}F_6$ complexes in a similar way. Remember that the $LiSbF_6$ and $KOsF_6$ crystal structures are typical for compounds containing small and large countercations, respectively (Hepworth *et al.*, 1956; Burns, 1962; Babel, 1967). In this case, $LiSbF_6$ transforms into the $KOsF_6$ structure type either owing to the instability of the packing of the complex ions, caused by the low occupancy of the voids, or because of the allocation of large cations in the voids (Fig. 1). The increase in the structure-forming role with increasing cation size can also be caused by the decrease in cation screening and, hence, by the preference of the cationic sublattice to be highly uniform owing to the increased electrostatic repulsions.

4.5.2. Cation charge. To separate the charge effect one needs to find a series of compounds, containing chemically identical countercations in different oxidation states. Unfortunately, there are no such series in the sample, thus the structure-forming effects caused by cation charge cannot be isolated from cation size factors. However, while analysing the

crystal structure of the concrete compound the effect is clear in most cases. Let us consider as an example how the uniformity of different cationic sublattices varies in the $M1^{I}{}_2M3F_6$, $M1^{I}M2^{II}M3F_6$ and $M1^{I}M3F_6$ compound series with ordered cations (Figs. 2*a*–*c*). In the morphotropic series, G_3 values indicate that the nature of the structure-forming sublattice does not influence the charge effect: complexing ion arrays are more uniform than the arrays of countercations, because G_3 values for the {*M*3} sublattices are smaller, as a rule. Since the same regularity is kept all over the sample, one can state that a high ion charge facilitates the structure-forming capability of the ion. The $M1^{II}M3F_6$ crystal structures (Fig. 2*c*) are clear examples of the co-influence of the size and charge of cations on their structure-forming capability. If $M1^{II}$ cations are small the sublattice of the complexing atoms is the most uniform, otherwise the 'inversion' of G_3 values for the {*M*1, *M*3} and {*M*3} sublattices takes place.

An interesting example of a highly charged ion playing an essential structure-forming role is the garnet structure type, where the sublattice of the complexing atoms has the topology of the ideal b.c.c. sublattice (Table 1). Earlier the b.c.c. motif was found in garnet by O'Keeffe (1977), who considered this crystal structure as a b.c.c. packing of rods, formed by alternate octahedra and trigonal prisms whose frameworks are based on F^- ions. The octahedra in each rod are filled with M^{III} cations, whereas the trigonal prisms are empty. It is the $M3^{III}$ cations that seem to predetermine the b.c.c. motif of rods, because $M1^{I}$ and $M2^{I}$ cations occupy voids between the rods. This fact allows the interpretation of the garnet crystal structure in two different ways. First, it can definitely be stated that the *M*3 cation is a separate structural unit, since the b.c.c. sublattice is typical of the uniform arrangement of points (§2.5). In this case, the garnet crystal structure should be described as a packing of fluoride ions. Second, the garnet crystal structure can be interpreted as a packing of complex groups, keeping in mind that the octahedra [$M3F_6$] look like deformable spheres owing to their non-sphericity. Peresypkina & Blatov (2000*a*,*b*, 2002) have shown that the packings of non-spherical particles allow deviations from close packings and often have the b.c.c. topology.

4.5.3. Polymorphism. In the context of the approach used, the phase transitions in complex fluorides can be explained as changes in the uniformity and structure-forming role of various ionic sublattices. An increase in pressure and/or temperature is known to be structurally equivalent to an increase in effective ionic sizes and charges. Blatov & Serezhkin (2000) have shown that in high-temperature or high-pressure phases the crystal structure becomes more uniform, as a rule. It was interesting to consider how these factors influence the crystal structure of complex fluorides.

Thermal polymorphism. At present there are a few experimental studies on thermal polymorphism for 3*d* metal complex fluorides. In this section all such examples will be considered together with the temperature influence on the uniformity of ionic sublattices and their topological properties.

Recently Gorev *et al.* (1997) and Flerov *et al.* (2002) have studied phase transitions for the Rb_2KScF_6 elpasolite, which is cubic under standard conditions (Table 1). When cooling its ideal cubic structure distorts to tetragonal (space group $I4/m$) and then to the monoclinic cryolite structure (space group $P2_1/c$). Note that the latter structure investigation had R_f = 6.4%, therefore, this phase is missing in the sample studied, but here it will be considered to complete the transition sequence of the compound. Investigating the Rb_2KScF_6 phase transitions Flerov *et al.* (1998, 2002) stated that the structural distortions were caused by insufficient tilts of ScF_6 and KF_6 octahedra, which were almost undistorted. Thus, the tilt of the octahedra out of one of three main cubic axes leads the cubic structure to tetragonal distortion, whereas arbitrary tilts lead to the monoclinic cryolite structure. During the phase transitions the entropy changes are small and in good agreement with minor structure changes. Let us consider this polymorph sequence in terms of the uniformity of ionic sublattices. In Table 4, G_3 values are given for the three phases. When compared the data indicate the following conclusions:

(i) The packing of $\{Rb^+, F^-\}$ becomes more uniform at the $P2_1/c \rightarrow I4/m \rightarrow Fm\bar{3}m$ transition. An increase in temperature consecutively leads to a higher mobility of ions, an increase in their effective sizes and, hence, to their higher structure-forming capability that in turn causes the uniformity increase for the mixed packing.

(ii) The topological properties of ionic sublattices, except the fluoride sublattice, remain unchanged. This fact confirms the phase transition mechanism leading to tilts of octahedra in the eplasolite crystal structure, *i.e.* the displacement of fluoride ions only relative to the fixed centroids (K^I and Sc^{III} cations) of these polyhedra.

(iii) The uniformity of the fluoride sublattice decreases, which clearly demonstrates the mechanism of the phase transition found by Flerov *et al.* (2002).

Note that although Rb_2KScF_6 undergoes phase transitions, sequential reorganization of its crystal structure does not influence the main structure-forming components, in particular, the sublattice of highly charged scandium cations and the complete cationic sublattice. They keep their geometric motifs undistorted and are favourable in terms of packing and the spatial arrangement of points. Besides, according to Flerov *et al.* (1998, 2002), the mechanism of phase transitions based on tilts of $M1F_6$ octahedra is typical for various elpasolites with monatomic countercations. This fact proves the general tendency of elpasolites to be stabilized by the formation of highly uniform ionic sublattices {*M*3} and {*M*1, *M*2, *M*3}.

Another example is the thermal polymorphism of Cs_2NaTiF_6. The compound exists as rhombohedral (Becker & Hoppe, 1974) and trigonal (Alter & Hoppe, 1989) phases. In the crystal structure of the trigonal high-temperature phase there are {*M*3} and {*M*1, *M*2, M3} structure-forming sublattices; in the rhombohedral phase the complete cationic sublattice is no longer structure-forming. The phase transition was not studied in this case; however, its mechanism obviously differs from the mechanism described above since both phases are multi-layered cationic–anionic packings with different sequences of layers (Table 1). When heated the 12-layered packing rebuilds to form the six-layered packing. This struc-

tural change is accompanied by a slight increase in the uniformity of mixed packing, fluoride and complete cationic sublattices (Table 5).

It is of interest to consider the α–β dimorphism of $LiMnFeF_6$, because in this case the changes of the crystal structure affect not so much the structure-forming component of the structure, which remains a packing of fluoride ions, but rather the cationic sublattice. During the transition from the α- to the β-phase (structure types of Na_2SiF_6 and $LiMnGaF_6$, respectively; Table 1, Fig. 1), lithium and iron cations trade places. Courbion *et al.* (1982) noted a small change in the Coulomb energy during the phase transition that was in good agreement with the reversible character of the transition. Note that a more uniform arrangement of iron cations is realised in the cationic framework of the β-phase. The reason for the dimorphism in this case is likely to be the preference of highly charged iron cations to arrange with a reduction in their repulsion energy. Therefore, Fe^{3+} cations occupy the very positions that arrange the most uniformly in the space available; this arrangement is close by uniformity to the structure-forming fluoride sublattice. This example demonstrates that a temperature increase provides an increase in uniformity of the highly charged cationic sublattice. Note that not only structure-forming sublattices, but most of ionic sublattices become more uniform in high-temperature phases (Tables 4 and 5).

High-pressure polymorphism. The change in structure type without changing the structure-forming motif is typical for compounds with small cations (for instance, $LiMnFeF_6$). Migrating from one position to another, they need to overcome a small energy barrier and therefore the initial motif of structure-forming packing remains unchanged or changes slightly. However, if the countercations are large, new structure-forming components appear and the structure type changes. Let us concentrate on the well known and carefully studied fluoroelpasolite family $M1_2M2M3^{III}F_6$, $r(M1) > r(M2) > r(M3)$. Most of the elpasolites are known to exist as two polymorphs with space groups $R\bar{3}m$ and $Fm\bar{3}m$ (Winkler, 1953; Babel & Haegele, 1976). Using the Goldschmidt tolerance factor (Babel, 1967; Massa & Babel, 1988; Flerov *et al.*, 1998)

$$t = 2^{1/2}\left[(r_{M1} + r_F)/(r_{M2} + r_{M3} + 2r_F)\right], \qquad (5)$$

one can determine whether the modification is stable. Under standard conditions, when $t < 1$, the stable phase is cubic; otherwise it is rhombohedral. The transition from one phase to another corresponds to the critical value $t = 1$, when cations are in contact with anions. The transition becomes possible when pressure increases [for instance up to 5 kbar for Cs_2NaMnF_6 (Massa, 1982)] or when temperature decreases. In particular, if $t \geq 1$ the rhombohedral phase can be transformed into cubic only at high pressure (Graulich *et al.*, 1992). While studying high-pressure phase formation, Graulich *et al.* (1992) found the so-called 'distance–pressure' paradox when the $M1-F$ bonds in $[M1F_6]$ octahedra were unexpectedly shortened, the $M2-F$ bonds were lengthened and the $M3-F$ bonds were lengthened slightly. The same regularity was revealed for the transition from a high- to a low-temperature phase. At first sight it looks strange that the largest cation $M1$ strongly compressed by its environment in the rhombohedral phase undergoes an additional compression in the crystal structure of cubic high-pressure phases. Graulich *et al.* (1992) explained the possibility of the phase transitions and changes in interatomic distances in terms of changing the t value at various ambient conditions. Let us consider this phenomenon and analyse the high-pressure dimorphism of elpasolite family fluorides within the framework of our approach. Four compounds with the appropriate value $t = 1.024$ are present in the sample (Massa, 1982), but only for two of them are the polymorphs well studied, namely for α- and γ-Cs_2NaM3F_6 ($M3$ = Fe, Mn). For both polymorphs the $Cs-F$ bonds are shortened in $[M1^IF_6]$ and $[M2^IF_6]$ octahedra, whereas the $Na-F$ bonds are elongated by 0.10–0.15 Å. At the same time, G_3 values show essentially different structure organization of these compounds. Under normal pressure the γ-phase of the structure-forming sublattice is composed of complex ions, whereas the high-pressure α-phase is based on the complete cationic sublattice. In our opinion, the tendency of large cations to be compressed is caused by the structure-forming cationic sublattice appearing. At high pressure, the sublattice tends to minimize cation–cation interactions and reach a favourable uniform spatial arrangement (Blatov & Serezhkin, 2000). This is why the cationic sublattice is ideal b.c.c. both in this case and in crystal structures of all 32 cubic elpasolites of the sample (including tetragonally distorted Rb_2KScF_6) for both high-pressure and low-temperature phases. Note that even in the Cs_2KMnF_6 crystal structure (Schneider & Hoppe, 1970) the cationic sublattice, which is tetragonally distorted owing to the Jahn–Teller effect, also has b.c.c. topology. It keeps high uniformity ($G_3 = 0.0786$) and is slightly distorted compared with the ideal b.c.c. lattice.

Another example is the Li_2CrF_6 phase synthesized at 300 kbar (Siebert & Hoppe, 1972), which belongs to the Na_2SnF_6 structure type. In this compound with small countercations, the structure-forming role of complexes is found (Table 1). Let us emphasize that this structure type is a monoclinic distortion of the widespread trigonal Na_2SiF_6 type based on fluoride h.c.p. (Siebert & Hoppe, 1972). As the high-pressure polymorphism of Li_2CrF_6 has not been studied, one can assume that at normal pressure Li_2CrF_6 may crystallize in the Na_2SiF_6 type. High pressure results in an increase in the coordination numbers of fluoride ions of up to 13; their packing loses the hexagonal motif of the initial trigonal structure type and strives for b.c.c. because the topology of the fluoride sublattice ($N_{1-3} = \{13, 49, 110\}$) becomes closer to the b.c.c. motif. This process leads the initial fluoride structure-forming packing to distort and a new structure-forming motif to appear. Since small lithium cations cannot stimulate leading cationic sublattices to appear, complex ions form new structure-forming packing. New packing can be more favourable for the high-pressure phase as the packing of multiatomic particles should be more deformable than the packing of fluoride ions. Note that the assumption concerning the structure type of the normal-pressure Li_2CrF_6 phase is in good agreement with the fact that even in the structure types

occurring for compounds with medium-sized $M1^{I}$ = Na ions (Babel, 1967; Massa & Babel, 1988), distorted fluoride h.c.p is still stable and distorted by only 4–8% of its G_3 value in comparison with ideal h.c.p. For the fluorides with $M1^{I}$ = K the topological h.c.p. motif disappears (Table 1), giving way to mixed cationic–anionic packing and/or the packing of complex ions.

Thus, high-pressure polymorphism causes an increase in cationic sublattice uniformity and, hence, an increase in their structure-forming capability.

4.6. Topological properties of cationic sublattices

It is worth paying attention to the topological features of cationic sublattices irrespective of their structure-forming role in crystal structures. Recently O'Keeffe & Hyde (1985), Vegas *et al.* (1991) and Vegas & Jansen (2002) found that the cations allocated to the voids of anionic packing played an active role while forming ionic crystal structures. Vegas *et al.* (1991) noted that cationic sublattices in the $M1_nM2_mX_z$ compounds kept the motif similar to the high-pressure intermetallic $M1_nM2_m$ phases; hence, the anions compressed the cationic sublattice like ambient pressure. It seems that the same effects cause the topological similarity of cationic sublattices in the crystal structures of complex fluorides belonging to modified pyrochlores and in the intermetallic Laves phase $MgCu_2$ (see §4.3). Thus, it is interesting to study the aforementioned similarity between the topological properties of binary compounds and cationic sublattices in the crystal structures of fluorides, including cations with rather different sizes and charges. To reach rather uniform spatial arrangement, the complete cationic sublattice should not necessarily be structure-forming. The striving towards the maximum possible uniformity is typical of any sublattice of cations because of their mutual repulsion, but independent of their ability to predetermine the crystal structure. However, this tendency becomes apparent differently in various compounds, therefore, the sublattices with weak structure-forming roles are less uniform, but can be of the same topology as their highly uniform analogue. For instance, cationic sublattices in the crystal structures of fluorides of the colquiriite type and of $LiCdCoF_6$ are similar to those in binary intermetallides Ni_2Th and Al_2Th, respectively (Brown, 1961). Note that in this case cations play no structure-forming role; the cationic sublattice is characterized by G_3 = 0.0823, which is equal to the G_3 value of intermetallide crystal structures within $\sigma(G_3)$. Besides, there are cationic sublattices in the fluorides investigated, whose topologies coincide with the topologies of ion arrangements in ionic binary compounds. For instance, in the crystal structure of $NaSrFeF_6$ (Hemon & Courbion, 1992) the cationic sublattice is topologically equal to the cationic–anionic sublattice in the cotunnite ($PbCl_2$) crystal structure [G_3(Pb,Cl) = 0.0809] and is slightly less uniform (Table 1). The cationic sublattice in the crystal structure of β-$LiMnFeF_6$ is topologically similar to the crystal structure of the high-temperature form of θ-Ni_2Si [G_3(Ni,Si) = 0.0791, Table 1].

5. Conclusions

5.1. Crystal structure prediction for $M1_nM2_mM3F_6$ 3*d* metal complex fluorides

Following the regularities based on the concept of the uniform ionic sublattice, it can be stated as a result of the analysis of 139 $M1_nM2_mM3F_6$ inorganic complex fluorides that:

(i) Anions (or anions together with similar-sized cations) form a packing where all atoms contact each other; other cations occupy voids in the packing. The preference towards the maximum uniform arrangement of the ions leads the packing to one of the close-packing motifs.

(ii) Cations tend to arrange in the voids of the packing in the most uniform manner. This tendency results in a b.c.c. cationic sublattice with the minimum G_3 value.

(iii) The more uniform the arrangement of ions in crystal structure (*i.e.* the smaller the G_3 for their sublattice), the stronger their structure-forming role is marked.

(iv) The larger the ion, the higher the ionic charge and the structure-forming capability of the ion in the crystal lattice (*i.e.* the smaller G_3 value for their sublattice).

Some of the regularities are well known in crystal chemistry, but taken together they allow good prediction of the structural features of complex fluorides which have not structurally been characterized or have not yet been obtained. It is the use of G_3 criteria and coordination sequences that enables these regularities to be regarded as quantitative and to apply them to predict structural features for new $M1_nM2_mM3F_6$ compounds (Table 6). The following rules resulting from these regularities should be used:

(i) If a compound contains small *M*1 and *M*2 cations with a low structure-forming capability, such as Na^+ and Li^+, it should be based, with high probability, on a distorted packing of fluoride ions with the topological motif of one of the close packings.

(ii) On the contrary, this motif should not occur if a complex fluoride contains large *M*1 and/or *M*2 cations, when either the complete cationic sublattice or packing of complexes stabilize the crystal structure.

(iii) A cationic sublattice similar to atomic packings in intermetallide alloys is favourable in terms of the local mutual arrangement of the cations with different charges.

(iv) Large cations strive to form a b.c.c. sublattice.

(v) The sublattice of cations with the highest charge is usually the most uniform cationic sublattice.

(vi) The crystal structures with the leading role in cationic frameworks allow either packing of fluoride ions or mixed cationic–anionic packing.

This study was financially supported by the Russian Foundation for Basic Research (projects 01-07-90092 and 02-07-06004). Authors are grateful to Dr N. V. Podberezskaya for productive discussions of all the main parts of this work.

References

Alter, E. & Hoppe, R. (1989). *Z. Anorg. Allg. Chem.* **579**, 16–26.
Babel, D. (1967). *Structure and Bonding*, Vol. 3, pp. 1–87. Berlin: Springer Verlag.
Babel, D. & Haegele, R. (1976). *J. Solid State Chem.* **18**, 39–50.
Becker, S. & Hoppe, R. (1974). *Z. Anorg. Allg. Chem.* **403**, 127–136.
Blatov, V. A. (2000). *Acta Cryst.* A**56**, 178–188.
Blatov, V. A. (2001). *Z. Kristallogr.* **216**, 165–171.
Blatov, V. A. & Serezhkin, V. N. (2000). *Russ. J. Inorg. Chem.* Suppl., S105–S220.
Blatov, V. A., Shevchenko, A. P. & Serezhkin, V. N. (2000). *J. Appl. Cryst.* **33**, 1193.
Blatov, V. A. & Zakutkin, Yu. A. (2002). *Z. Kristallogr.* **217**, 464–473.
Bokii, G. B. (1971). *Crystal Chemistry.* Moscow: Nauka (in Russian).
Borisov, S. V. (2000). *Cryst. Rep.* **45**, 709–713.
Borisov, S. V. & Podberezskaya, N. V. (1984). *Stable Cationic Frameworks in Crystal Structures of Fluorides and Oxides.* Novosibirsk: Nauka (in Russian)
Brown, A. (1961). *Acta Cryst.* **14**, 860–865.
Brunner, G. O. & Laves, F. (1971). *Wiss. Z. Tech. University Dresden.* **20**, 387–390.
Burns, J. (1962). *Acta Cryst.* **15**, 1098–1101.
Carlson, S., Xu, Y. & Norrestam, R. (1998). *J. Solid State Chem.* **135**, 116–120.
Convay, J. H. & Sloane, N. J. A. (1988). *Sphere Packings, Lattice and Groups.* Berlin: Springer-Verlag.
Courbion, G., Jacoboni, C. & De Pape, R. (1982). *J. Solid State Chem.* **45**, 127–134.
Englich, U. & Massa, W. (1992). *Acta Cryst.* C**48**, 6–8.
Flerov, I. N., Gorev, M. V., Aleksandrov, K. S., Tressaud, A., Grannec, J. & Couzi, J. M. (1998). *Mater. Sci. Engng*, **24**, 81–151.
Flerov, I. N., Gorev, M. V., Grannec, J. & Tressaud, A. (2002). *J. Fluorine Chem.* **116**, 9–14.
Frank, F. C. & Kasper, J. S. (1958). *Acta Cryst.* **11**, 184–190.
Gorev, M. V., Flerov, I. N., Tressaud, A. & Grannec, J. (1997). *Phys. Solid State*, **39**, 1647–1651.
Graulich, J., Drüeke, St. & Babel, D. (1992). *Z. Anorg. Allg. Chem.* **624**, 1460–1464.
Hemon, A. & Courbion, G. (1992). *Eur. J. Solid State Inorg. Chem.* **29**, 519–531.
Hepworth, M. A., Jack, K. N. & Westland, G. J. (1956). *J. Inorg. Nucl. Chem.* **2**, 79–87.
Herdtweck, E., Massa, W. & Babel, D. (1986). *Z. Anorg. Allg. Chem.* **539**, 89–94.
Hoppe, R. & Hofmann, B. (1977). *Z. Anorg. Allg. Chem.* **436**, 65–74.
Inorganic Crystal Structure Database. (2001). Gmelin Institut für Anorganische Chemie and Fiz Karlsruhe.
Kemmitt, R. D. W., Russell, D. R. & Sharp, D. W. A. (1963). *J. Chem. Soc.* pp. 4408–4413.
Massa, W. (1982). *Z. Anorg. Allg. Chem.* **491**, 208–216.
Massa, W. & Babel, D. (1988). *Chem. Rev.* **88**, 275–296.
O'Keeffe, M. (1977). *Acta Cryst.* A**33**, 914–923.
O'Keeffe, M. (1995). *Z. Kristallogr.* **210**, 905–908.
O'Keeffe, M. & Hyde, B.G. (1985). *Structure and Bonding*, Vol. 61, pp. 77–144. Berlin: Springer Verlag.
Ohba, T., Kitano, Y. & Komura, Y. (1984). *Acta Cryst.* C**40**, 1–5.
Pauling, L. (1927). *J. Am. Chem. Soc.* **49**, 765.
Peresypkina, E. V. & Blatov, V. A. (2000*a*). *Acta Cryst.* B**56**, 501–511.
Peresypkina, E. V. & Blatov, V. A. (2000*b*). *Acta Cryst.* B**56**, 1035–1045.
Peresypkina, E. V. & Blatov, V. A. (2002). *Z. Kristallogr.* **217**, 91–112.
Schneider, S. & Hoppe, R. (1970). *Z. Anorg. Allg. Chem.* **376**, 268–276.
Sekino, T., Endo, T., Sato, T. & Shimada, M. (1990). *J. Solid State Chem.* **88**, 505–512.
Shannon, R. D. & Prewitt, C.T. (1969). *Acta Cryst.* B**25**, 925–946.
Siebert, G. & Hoppe, R. (1972). *Z. Anorg. Allg. Chem.* **391**, 113–116.
Vainshtein, B. K., Fridkin, V. M. & Indenbom, V. L. (1983). *Modern Crystallography*, Vol. 2. Berlin: Springer-Verlag.
Vegas, A. & Jansen, M. (2002). *Acta Cryst.* B**58**, 38–51.
Vegas, A., Romero, A. & Martinez-Ripoll, M. (1991). *Acta Cryst.* B**47**, 17–23.
Viebahn, W. (1971). *Z. Anorg. Allg. Chem.* **339**, 335–339.
Wells, A. F. (1986). *Structural Inorganic Chemistry.* Oxford: Clarendon Press.
Winkler, H. G. F. (1953). *Acta Cryst.* **7**, 33–40.